Data-Driven Resource Management for Ultra-Dense Small Cells: An Affinity Propagation Clustering Approach

Li-Chun Wang, *Fellow, IEEE,* and Shao-Hung Cheng, *Student Member, IEEE*

Abstract—Deploying dense small cells is the key to providing high capacity, but raise the serious issue of energy consumption and inter-cell interference. To understand the behaviors of ultra-dense small cells (UDSC) with dynamic interference and traffic patterns, this paper presents a data-driven resource management (DDRM) framework to implement power control and channel rearrangement in UDSC. We find that the inter-cell interference can be used to describe the affinity of cells. Thus, we propose an unsupervised learning algorithm for UDSC, called affinity propagation power control (APPC) mechanism. In principle, APPC first groups small cells into different clusters and identifies cluster centers. Next, the transmission power of a cluster center is decreased to reduce the interference to the neighboring cells' users in this cluster. Since lowering transmission power of a cluster center cell may cause the performance degradation to the users at the cell edge, a victim-aware channel rearrangement (VACR) mechanism is further designed to adjust the channel usage bandwidth of the neighboring cells in order to guarantee the quality of service of these victimized users. Our simulation results show that the DDRM framework can significantly improve energy efficiency and throughput in UDSC compared to the existing approaches.

Index Terms—Affinity propagation clustering, data-driven, ultra-dense small cells, energy efficiency, quality of service

1 Introduction

Ultra-dense small cells (UDSC) are the key to providing high capacity for the fifth generation (5G) mobile systems [1]. Unlike macrocells can be deployed by the help of cell planning tools, small cells are usually installed in an ad hoc manner, thereby making real-time interference management in UDSC challenging [2]. Because customers' traffic loads change in both time domain and spatial domain, underutilized small cells lead to the issue of spectrum and energy inefficieny. Hence, the benefits of high capacity and coverage extension of UDSC come at a price. The operation cost of UDSC is high. Complex interference and dynamic traffic situations make quality of service (QoS) of UDSC difficult to maintain.

In the literature, most of the existing UDSC papers tackled the maximization issues of spectrum efficiency and energy efficiency by using game theoretic approaches [3], [4], [5]. A novel utility function was proposed to integrate spectrum efficiency and energy efficiency [3]. An interference-aware energy efficiency maximization problem for UDSC was solved by using a bargaining cooperative game approach [4]. In [5], a distributed power control game model was designed to maximize the sum rate of UDSC. However, in the above game theoretical approaches, the effects of dynamic cell switching on/off, time-varying user density, and frequently changed interference have not been considered yet.

In this paper, we propose a joint interference-and-traffic aware data-driven learning approach to manage the non-uniformly distributed traffic loads and the frequently changing interference in small cells. Data-driven approaches start from collecting data. Then data analysis techniques are utilized to extract the knowledge and understand the behaviors of a complex system in a dynamic environment. The huge volume of data help overcome the difficulty of modeling a complex system [6]. Data analysis techniques consist of data mining and machine learning. The former technique is to discover knowledge by understanding the complex relationships between data, and the later technique aims at providing the ability to recognize knowledge automatically [6]. A general vision of data-driven learning approaches to provide self-organizing networks (SON) for 5G mobile networks was given in [7].

1.1 Motivation

The opportunities of applying machine learning algorithms to small cells, large-scale MIMO, cognitive radio, and device-to-device communication were discussed in [8], but without going details on each function. Supervised learning, unsupervised learning, and reinforcement learning have different applications in wireless networks. First, supervised learning is suitable for wireless network problems assuming that the prior labeled data are available [6]. Supervised learning aims to build a system performance prediction model. Second,

• *The authors are with the Department of Electrical and Computer Engineering, National Chiao Tung University, Taiwan 300, China. E-mail: lichun@cc.nctu.edu.tw, locoling@gmail.com.*

Manuscript received 7 Feb. 2018; revised 19 Apr. 2018; accepted 24 May 2018. Date of publication 29 May 2018; date of current version 11 Sept. 2019. (Corresponding author: Li-Chun Wang.) Recommended for acceptance by J. Tang. For information on obtaining reprints of this article, please send e-mail to: reprints@ieee.org, and reference the Digital Object Identifier below. Digital Object Identifier no. 10.1109/TNSE.2018.2842113

unsupervised learning is used for wireless network problems without the prior labeled data [6]. Unsupervised learning needs to find the hidden structures of the observed data. Finally, reinforcement learning aims to optimize the system performance based on the interaction of an agent in the considered environment [8].

Intuitively, the total system interference in the UDSC can be reduced by lowering the transmission power of the high interference cells. However, too many low power cells will decrease the total system throughput. Thus, how to determine the appropriate number of low power cells in UDSC is an interesting research problem. In our previous work [9], a base station data-driven supervised learning method was proposed to model the throughput performance of UDSC, taking into account of dynamic interference and nonuniform traffic loads. It assumes that the labeled throughput data for a set of system parameters is available. Here, a set of system parameters include the number of users and the transmission power in each small cell. However, such a prior knowledge is usually unavailable. For instance, because indoor small cells are operated in a plug-and-play manner, it is difficult to obtain the aforementioned labeled data. According to [6], unsupervised learning can be used to find the hidden structure of unlabeled data. It can save the time of collecting labeled data and training model. To our best knowledge, an unsupervised learning approach in UDSC with emphasis on both interference reduction and energy saving is missing in the literature.

We observe that the inter-cell interference can be utilized to evaluate the affinity between pairs of small cells. Thus, grouping small cells into different clusters can help understand the complex interference between cells. The center cell in each cluster causes the most serious interference to the customers of other neighboring member cells. Therefore, the transmission power of the center cell of a cluster needs to be decreased. Because the interference conditions in UDSC dynamically change due to user mobility, the automation of selecting cluster centers is necessary. The main challenge for this problem lies in the fact that the number of clusters is also an unknown parameter. Thus, the K-mean clustering approach is not suitable for UDSC in dynamic environments since the number of clusters (i.e., K) is assumed to be known [10]. To this end, we adopt the affinity propagation clustering approach [11] to infer the number of clusters, cluster size, and cluster center automatically.

1.2 Objectives and Contributions

In this paper, we aim at improving the total cell throughput and energy efficiency of the plug-and-play UDSC. By observing the operation data of each cell, we develop a data-driven resource management (DDRM) framework with affinity propagation power control (APPC) and victim-aware channel rearrangement (VACR) mechanisms. The contributions of this paper are described as follows.

- We design an unsupervised learning affinity propagation algorithm for the plug-and-play UDSC to find the hidden interference structures, utilizing the input data of transmission power and the reference signal received power. The interference structure can be represented by the cluster center and the cluster members in each cluster. Without the need for offline training and labeled data, affinity propagation algorithm is suitable for the plug-and-play small cells.
- A power control mechanism called APPC is proposed to 1) group small cells into different clusters; 2) determine the proper cluster centers; 3) lower transmission power of the cell of the cluster center to reduce the interference to the non-served users of other cells in each cluster.
- We develop a VACR mechanism to improve the signal quality of edge users after lowering the transmission power of the center cell of the cluster. The VACR mechanism can identify the victimized users (i.e., low received signal and high interference strength) and rearrange channel of neighboring cells to avoid interfering the victimized users.

Our simulation results show that the proposed DDRM framework with power control and channel rearrangement can enhance energy efficiency and throughput in the plug-and-play UDSC scenario, compared to the existing approach. In our previous work [12], we only designed power control process for enhancing the energy efficiency of UDSC, but sacrifice the QoS of the users at the cell edge.

1.3 Organization

The remaining parts of this paper are organized as follows. In Section 2, we give a brief review of related works. Section 3 describes the system architecture, radio propagation model, performance metrics, and problem formulation. Section 4 illustrates the proposed DDRM framework. The APPC and VACR mechanisms are detailed in Sections 5 and 6, respectively. Simulation results are discussed in Section 7. Finally, this paper is concluded in Section 8.

2 Related Work

In the literature, [13], [14], [15], [16] designed the clustering approach to perform resource allocation for interference mitigation in UDSC. In [13], based on interference-based clustering, subchannel assignment, and power allocation, the authors proposed an interference management scheme to maximize the total throughput of all users in femtocells, but energy efficiency issue is not addressed. In [14], the distance-based clustering downlink resource allocation mechanism was proposed to maximize the overall system capacity of small cells. The authors of [15] designed a novel hierarchical resource allocation framework, which includes distributed clustering, intra-cluster subchannel allocation, and power adjustment, to address the downlink co-tier interference problem in hyper-dense small cell networks. A semi-clustering approach for victim cells was presented to manage the interference of ultra-dense femtocell networks [16]. A signal-based clustering power saving algorithm for small cells with sleep mode was investigated in [17]. Furthermore, [18] applied the affinity propagation clustering and the artificial neural network to classify the indoor and outdoor users in femtocell networks. To our knowledge, a clustering-based resource allocation simultaneously considering interference mitigation and energy saving is missing in the literature for plug-and-play UDSC, especially in a dynamic and nonuniform traffic load environment.

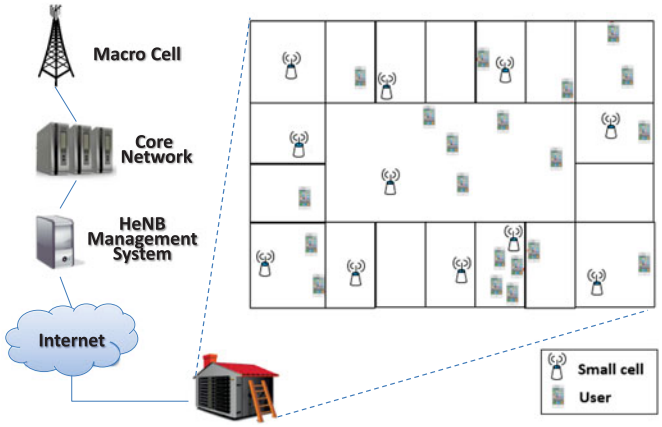

Fig. 1. A deployment scenario of the ultra-dense small cells (UDSC).

3 System Model and Problem Formulation

3.1 System Architecture

The downlink UDSC with co-tier interference are randomly deployed in an indoor area, as shown in Fig. 1. The indoor small cells are considered as the plug-and-play customer premise devices, which are called the home eNodeBs (HeNBs) in 3GPP LTE standard. Usually, the coverage of small cells in home or enterprise are limited. As shown in the figure, HeNB management system (HMS) connects to each small cell, which acts as a central controller to collect the information from all the small cells and to provide a function of automatically setting the operating parameters for self-healing and self-optimization [19], [20]. We assume that each small cell is equipped with only one isotropic antenna, uses unique cell-IDs, and can serve multiple customers with different user-IDs.

In addition, the active users are generated by a two-dimensional Poisson point process in the UDSC as [21]

$$\Pr\{M = m|a\} = \frac{(\lambda_u a)^m}{m!} e^{\lambda_u a}, \tag{1}$$

where the random variable M represents the number of active users in a square area a, and λ_u is the user density.

3.2 Radio Propagation Model

In this paper, we consider two radio propagation effects, i.e., shadowing and path loss. Shadowing (denoted by ψ) is modeled by a log-normal distributed random variable. That is, $10log_{10}\psi$ is a normal random variable with zero mean and standard deviation σ_ψ. Let $RSS_{q,n}$ represent the received signal strength (RSS) of user n from the small cell q, and $P_{tra,q}$ represent the transmission power for user data from a small cell q. Then we have

$$RSS_{q,n} = P_{tra,q} D_{q,n}^{-\alpha} \psi, \tag{2}$$

where $D_{q,n}$ is the distance from cell q to user n, and α is the path loss exponent.

It is assumed that small cells can periodically transmit pilot symbols to obtain the measurement report of their connected users. Users scan the neighborhood to determine the physical cell identity (PCI) of neighboring small cells as well as the corresponding received pilot symbol signal strength (i.e., reference signal received power, RSRP). The RSRP at users' receiver are reported back to their serving cells. Then the information of RSRP of each small cell is collected by HMS, which can help the system schedule to allocate radio resource blocks and the transmission power. Therefore, the RSRP of user n from small cell q (denoted as $RSRP_{q,n}$) can be expressed as

$$RSRP_{q,n} = P_{ref} D_{q,n}^{-\alpha} \psi, \tag{3}$$

where P_{ref} is the transmission power of the pilot symbol signal. We assume that P_{ref} is equal to the maximum transmission power (i.e., 17 dBm).

3.3 Throughput, Link Reliability, and Fairness Index

The downlink signal to interference plus noise power ratio (SINR) from small cell q to user n, (denoted by $\Gamma_{q,n}$) can be written as

$$\Gamma_{q,n} = \frac{RSS_{q,n}}{\eta_0 + \sum_{k \neq q} RSS_{k,n}}, \tag{4}$$

where $RSS_{k,n}$ is the interfering signal strength from small cell k to user n, and η_0 is the thermal noise. We assume that each active user can utilize all the available bandwidth and each channel is fully loaded [22]. The throughput $r_{q,n}$ of user n from small cell q can be expressed

$$r_{q,n} = B_{q,n} \cdot \log_2(1 + \Gamma_{q,n}), \tag{5}$$

where $B_{q,n}$ is the allocated channel bandwidth to user n from cell q. Given B (the bandwidth) and M_q (the number of served users in the small cell q), the initial value of $B_{q,n}$ is set to $\frac{B}{M_q}$. Thus, the total cell throughput R_{tot} for Q small cells can be written as

$$R_{tot} = \sum_{q=1}^{Q} \sum_{n=1}^{M_q} r_{q,n}. \tag{6}$$

Then, we define the link reliability L_{rel} as the probability that the SINR Γ is higher than the required effective SINR threshold Γ_{th}

$$L_{rel} = \Pr\{\Gamma \geq \Gamma_{th}\}, \tag{7}$$

where the set $\Gamma = \{\Gamma_{q,n} |\ q = 1, 2, \ldots, Q;\ n = 1, 2, \ldots, M_q\}$.

To measure the fairness in terms of user throughput in the cluster center, we adopt Jain's fairness index [23]

$$\phi = \frac{(\sum_{n=1}^{M_c} r_{c,n})^2 M_c}{\sum_{n=1}^{M_c} {r_{c,n}}^2}, \tag{8}$$

where M_c is the number of served users and $r_{c,n}$ is the throughput of user n in the cluster center. Jain's fairness index ranges from $1/M_c$ (worst case) to 1 (best case).

3.4 Power Consumption and Energy Efficiency

In this paper, we assume that small cells can switch between active mode and sleeping mode for energy saving [24]. When a small cell does not serve any user, it will be switched to the sleeping mode. In this mode, a small cell can turn off the receiver module, including RF and power amplifier. By switching between active mode and sleeping mode based on the existence of active users, UDSC can improve its energy efficiency.

Referring to [25], we model the power consumption of small cell q (P_q) as

$$P_q = \beta_q \cdot P_{sle,q} + (1-\beta_q) \cdot P_{act,q}\ , \tag{9}$$

where $P_{sle,q}$ and $P_{act,q}$ are the consumed power in the sleeping mode and that in the active mode, respectively. $\beta_q = 1$ if small cell q is in the sleeping mode; otherwise, $\beta_q = 0$. Furthermore, $P_{act,q} = P_{bas} + \Delta \cdot P_{tra,q}$, where Δ is the power amplifier (PA) efficiency and P_{bas} is the basic circuit power consumption. Thus, the total power consumption P_{tot} of the system can be expressed as

$$\begin{aligned} P_{tot} &= \sum_{q=1}^{Q} P_q \\ &= \sum_{q=1}^{Q} \left[\beta_q \cdot P_{sle,q} + (1-\beta_q) \cdot (P_{bas} + \Delta P_{tra,q})\right]\ . \end{aligned} \tag{10}$$

In addition, we define the energy efficiency E_{eff} as the ratio of the total cell throughput R_{tot} over the total power consumption P_{tot}, i.e.,

$$E_{eff} = \frac{R_{tot}}{P_{tot}}\ . \tag{11}$$

3.5 Problem Formulation

To maximize the total system energy efficiency of UDSC, we formulate a joint power control and channel rearrangement optimization problem as follows:

$$\begin{aligned} \max\ & E_{eff} = \frac{\sum_{q=1}^{Q}\sum_{n=1}^{M_q} B_{q,n}\log_2(1+\Gamma_{q,n})}{\sum_{q=1}^{Q}[\beta_q P_{sle,q} + (1-\beta_q)(P_{bas}+\Delta P_{tra,q})]} \\ s.t.\quad & \mathrm{C1}: \beta_q \in \{0,1\}, \quad \forall q \\ & \mathrm{C2}: 0 < \sum_{q=1}^{Q} \beta_q \le Q \\ & \mathrm{C3}: H_i \cap H_j = \emptyset, \quad \forall H_i, H_j, \quad i \ne j \\ & \mathrm{C4}: 0 \le P_{tra,q} \le P_{tra,max}, \quad \forall q \\ & \mathrm{C5}: 0 < B_{q,n} \le B, \quad \forall q, \quad n \in U_q. \end{aligned} \tag{12}$$

In (12), C1 and C2 specify whether each cell is in the active mode or in the sleeping mode; C3 indicates that a small cell is belonged to one cluster, where H_i is cluster i; C4 is for the transmission power operation range; C5 is for the bandwidth limitation; $n \in U_q$ implies user n is served by small cell q.

4 Data-Driven Resource Management

The proposed DDRM framework aims to improve the system energy efficiency in UDSC. It is easy to model a complex system based on DDRM framework. Specifically, DDRM starts from collecting data. Then it utilizes the APPC and VACR algorithms to appropriately determine the transmission power and channel rearrangement in a dynamic environment. Cell ID, user ID, and RSRP are the required information to implement APPC and VACR algorithms. All this information can be obtained from the central controller HMS, which connecting to each small cell [26]. Fig. 2 shows the function blocks of our proposed DDRM framework for the plug-and-play UDSC for interference reduction and energy saving. In the following, we explain each function block in more details:

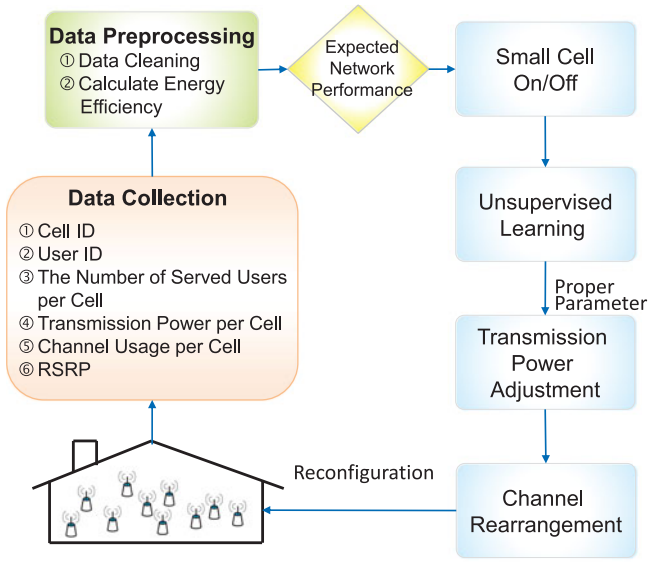

Fig. 2. The data-driven resource management (DDRM) framework is proposed to manage resource of the plug-and-play UDSC for interference reduction and energy saving.

- *Data collection:* The management interface between small cells and HMS is based on the standard TR-069. HMS can collect various kinds of operation data from UDSC, including the number of users, transmission power per small cell, RSRP, and so on.
- *Data preprocessing:* In this step, the irrelevant data (e.g., the preamble per cell) are removed and then the selected data are transformed into the required format for further data analysis. Based on the selected data including the cell ID, user ID, and RSRP from user's devices, the data can be transformed into the similarity matrix S (i.e., the interference relationship between the cells) for the APPC mechanism. Moreover, according to (10), the total power consumption P_{tot} can be obtained. Substituting the information of RSRP and the total power consumption P_{tot} into (6) and (11), the total cell throughput R_{tot} and energy efficiency E_{eff} can also be calculated. If the energy efficiency E_{eff} is lower than the default threshold, the DDRM framework will trigger power control and channel rearrangement based on the SON concept [7], [27].
- *Small cell on/off:* Users choose the serving cells according to RSRP. To save energy, power switched mechanism of each cell (i.e., active or sleeping mode) is determined based on whether there exist active users in the cell. For the cells with active mode after cell switching on/off, their transmission power can be determined by the APPC mechanism.
- *Unsupervised learning:* Affinity propagation clustering (i.e., one of the unsupervised learning techniques) is adopted to automatically determine the number of clusters and the corresponding cluster centers. Basically, the cluster center generates the strongest interference compared to other cluster members.

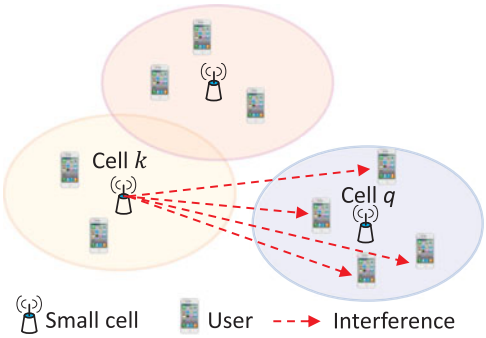

Fig. 3. The interference relationships $S(q,k)$ between one small cell k to the non-served users from the neighboring small cell q.

Therefore, the identities (ID) of the cluster centers are the input parameter to the next function block.

- *Transmission power adjustment:* According to the ID from the previous function block, the transmission power of the cluster centers is decreased to reduce interference. The APPC mechanism includes the affinity propagation clustering and transmission power adjustment, which can enhance the total cell throughput and energy efficiency for the plug-and-play UDSC.
- *Channel rearrangement:* After performing the APPC mechanism, the edge users of the cluster centers may have poor throughput. The VACR mechanism is designed to avoid interfering victimized users (i.e., low received signal and high interference strength) by rearranging channels used in the interfering cells. By doing so, the QoS of each user can be guaranteed in the plug-and-play UDSC.
- *System reconfiguration:* The DDRM framework can periodically reconfigure the resources of the plug-and-play UDSC (i.e., power levels and channels) to achieve the expected network performance.

5 Affinity Propagation Power Control

In this section, we discuss the affinity propagation clustering algorithm in the DDRM framework. Affinity propagation is a flexible, low-error, and simple clustering algorithm that takes the measures of similarity between pairs of objects as input data. The pairs of objects in the same cluster have the maximum similarity, while the objects in the different cluster have the minimum similarity [28]. Each cluster has a cluster center and all the objects are considered as potential cluster centers. However, the cluster center has larger similarity to cluster members in the same cluster. One advantage of affinity propagation is that the number of cluster center need not be specified beforehand. In the affinity propagation approach, the appropriate number of cluster centers emerges by passing messages between data points [11]. Messages between objects begin to transmit until a high-quality set of cluster centers and the corresponding clusters gradually emerges [29].

In many situations, objects are more easily characterized by a measure of pairwise similarities than the negative squared Euclidean distance. In this paper, we define the objects as the small cells and the similarities between objects as the inter-cell interference. We utilize the affinity propagation approach to find the interfering cells in the plug-and-play UDSC. The interfering cells which cause stronger interference should lower the transmission power to reduce interference and improve energy efficiency as well.

TABLE 1
Similarity Matrix for Five Small Cells Example

Small Cell ID	1	2	3	4	5
1	3	8	7	13	18
2	7	3	18	17	23
3	6	17	3	19	5
4	12	17	18	3	4
5	17	22	21	3	3

In our scenario, we consider the multiple users within a small cell. The similarity is defined as the interference relationships $S(q,k)$ between small cell k to multiple non-served users from the neighbor small cell q, as shown in Fig. 3. The interference relationship $S(q,k)$ represent the sum of the interference power. Then, we have

$$S(q,k) = \sum_{n \in U_q} P_{ref} D_{k,n}^{-\alpha} \psi = \sum_{n \in U_q} RSRP_{k,n}\ , \tag{13}$$

where $n \in U_q$ implies user n is served by small cell q and $RSRP_{k,n}$ is the reference signal received power of user n from the small cell k. Operation data from small cells are collected, including the cell ID, user ID, RSRP from user's devices, and so on. Substituting the information of RSRP into (13), the similarity $S(q,k)$ can be estimated. Let S denote the similarity matrix, where q and k refer to the rows and columns of the associated matrix.

To express the affinity propagation clustering algorithm, we simply utilize five small cells as an example. Actually, the algorithm can be applied to the general case with more multiple cells, which will be discussed in Section 7. The similarity matrix S in this example is shown in Table 1. The diagonal elements $S(k,k)$ of the matrix are called preferences and are selected from the off-diagonal elements. The preferences $S(k,k)$ will be set to the minimum of the input similarities (i.e., the off-diagonal elements) [30]. In this case, 3 (Unit: 10^{-10} watts) is the smallest value among the off-diagonal elements in Table 1. Thus, this value is placed in every entry of the diagonal elements. Notably, the similarity matrix S is an asymmetric matrix, which can not be implemented by the K-means clustering algorithm. However, the input matrix of affinity propagation can be either asymmetric or symmetric. Affinity propagation partitions small cells into clusters so that the intra-cluster interference is high and the inter-cluster interference is low. Compared with other small cells in the same cluster, the cluster center generates larger interference.

Unlike the K-means clustering, affinity propagation does not require to know the number of cluster centers. In affinity propagation, two messages passed between objects are 1) the responsibility value $R(q,k)$ from object q to candidate center k, and 2) the availability value $A(q,k)$ from candidate cluster center k to object q. The criterion value $C(q,k) = R(q,k) + A(q,k)$, which can identify the final cluster centers. Therefore, the affinity propagation clustering operates on

TABLE 2
Responsibility Matrix for Five Small Cells Example

Small Cell ID	1	2	3	4	5
1	-15	-10	-11	-5	5
2	-16	-20	-5	-6	5
3	-13	-2	-16	2	-14
4	-6	-1	1	-15	-14
5	-5	1	-1	-19	-19

TABLE 3
Availability Matrix for Five Small Cells Example

Small Cell ID	1	2	3	4	5
1	0	-19	-15	-13	-14
2	-15	1	-15	-13	-14
3	-15	-19	1	-15	-9
4	-15	-19	-16	2	-9
5	-15	-20	-15	-13	10

four matrices: a similarity matrix S, a responsibility matrix R, an availability matrix A, and a criterion matrix C [30]. To find appropriate cluster centers, these matrices are updated iteratively as follows:

$$R(q,k) = S(q,k) - \underset{k' \neq k}{max}\{A(q,k') + S(q,k')\} \ , \tag{14}$$

$$A(q,k) = min\{0, R(k,k) + \sum_{q' \notin \{q,k\}}^{Q_a} max\{0, R(q',k)\}\} \ , \tag{15}$$

$$A(k,k) = \sum_{q' \neq k}^{Q_a} max\{0, R(q',k)\} \ , \tag{16}$$

$$C(q,k) = R(q,k) + A(q,k) \ . \tag{17}$$

(14) is to compute the responsibility matrix R. The initial availability values $A(q,k')$ are set to zero. The responsibility value $R(q,k)$ reflects the accumulated evidence on how well-suited small cell k (column) is to serve as the cluster center for small cell q (row), taking into account other potential cluster centers k' for small cell q [11]. Based on similarity matrix S in Table 1, we calculate the responsibility matrix R as shown in Table 2. For example, the responsibility of small cell 2 (column) to small cell 1 (row) is -10, which is the similarity of small cell 2 to small cell 1 (i.e., 8) minus the maximum of the remaining similarities of the row of small cell 1 (i.e., 18). Note that the larger the value of $R(q,k)$, the more suitable the cluster center. $R(k,k) < 0$ because preferences $S(k,k)$ is set to the minimum of the input similarities.

(15) and (16) are used to update the off-diagonal and the diagonal elements of the availability matrix A, respectively. The availability value $A(q,k)$ reflects the accumulated evidence on how appropriate it would be for small cell q to pick small cell k as its cluster center, taking into account the support from other small cells q' [11]. Based on responsibility matrix R in Table 2, we obtain the availability matrix A as shown in Table 3. In (15), $\sum_{q' \notin \{q,k\}}^{Q_a} max\{0, R(q',k)\}$ is the sum of the nonnegative responsibility values $max\{0, R(q',k)\}$ for supporting cells q' to the candidate cluster center k. Because $R(k,k) < 0$, the set of q' do not include q and k in (15). For example, the availability of small cell 5 (column) to small cell 1 (row) is the self-responsibility of small cell 5 (i.e., -19) plus the sum of the remaining positive responsibilities of the column of small cell 5 excluding the responsibility of small cell 5 to small cell 1 (i.e., -19 + 5 + 0 + 0 = -14). From (16) the self-availability values $A(k,k)$ can be obtained based on the responsibilities from other small cells $q' \notin k$. For example, the self-availability of small cell 5 is the sum of the positive responsibilities of the column of small cell 5 excluding self-responsibility of small cell 5 (i.e., 5 + 5 + 0 + 0 = 10). Consequently, cell k is more well-suited for the cluster center of cell q when the availability value $A(q,k)$ is larger.

Using Equation (17) calculates the criterion matrix C which is as given in Table 4. The availabilities and responsibilities are combined to identify cluster centers [11]. For example, the criterion value of small cell 5 (column) to small cell 1 (row) is the sum of the responsibility and availability of small cell 5 to small cell 1 (i.e, 5 + -14 = -9). The column with the highest criterion value for each row identifies the cluster center for the item of that row. Repeat (14) through (17) until the solution is converged. In light of this, small cell 1, small cell 2, and small cell 5 constitute the first cluster and small cell 5 is selected to be the first cluster center. Then, small cells 3 and 4 constitute the second cluster. Small cell 4 is selected to be the second cluster center. Obviously, we find the cluster centers for this example with five small cells via affinity propagation.

According to the above discussion, affinity propagation can accumulate the responsibility values $R(q,k)$ and the availability values $A(q,k)$ to update the criterion $C(q,k)$ for the scenario in Fig. 1. The message-passing procedures can be terminated when the decisions stay constant after a certain number of iterations. When the messages are updated, it is important that they are damped to avoid numerical oscillations [11]. The function of the damping factor λ_{df} is to improve convergence when affinity propagation clustering fails to converge because of oscillations. Each availability values is set to $A(q,k) = \lambda_{df} \times A(q,k)' + (1 - \lambda_{df}) \times A(q,k)$, where $A(q,k)'$ is the previous iteration value and λ_{df} is between 0 and 1. In our experiments, the default damping factor is set to $\lambda_{df} = 0.5$. Observing the final convergent criterion matrix C leads to the results of the cluster and its cluster center. Finally, applying affinity propagation clustering produces high quality clusters with high intra-cluster similarity and low inter-cluster similarity. Because the similarity is the interference relationships $S(q,k)$, the cluster center generates larger interference to the non-served users from adjacent cells in the same cluster. Based on the above-mentioned reasons, we believe the cluster centers should decrease its transmission power (i.e., 17 dBm to 0 dBm) to reduce the interference and improve energy efficiency.

TABLE 4
Criterion Matrix for Five Small Cells Example

Small Cell ID	1	2	3	4	5
1	-15	-29	-26	-18	-9
2	-31	-19	-20	-19	-9
3	-28	-21	-15	-13	-23
4	-21	-20	-15	-13	-23
5	-20	-19	-16	-32	-9

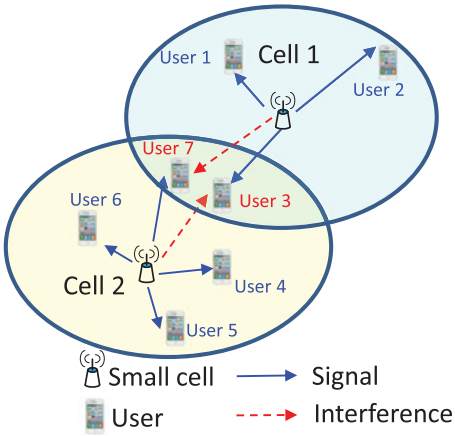

Fig. 4. User 3 is considered as the victimized user of small cell 2 and the user 7 is considered as the victimized user of small cell 1.

6 Victim-Aware Channel Rearrangement

In this section, we develop a VACR mechanism in the DDRM Framework. VACR aims to improve the throughput for the user in the plug-and-play UDSC. When a cell decreases its transmission power after performing APPC mechanism, its cell edge users will have poor throughput. The proposed VACR mechanism consists of the following four phases.

6.1 Phase 1: Service-Victim (SV) Matrix

The cell edge user experiences the serious interference from neighboring small cell when it is in the overlapping area between the cluster center and the neighboring cells. Victimized users are defined as the ones with low signal strength and high interference. The non-served user n is the victimized user of small cell q if the following inequality holds. That is

$$ISF_{q,k,n} = \frac{I_{q,n}}{S_{k,n}} = \frac{RSS_{q,n}}{RSS_{k,n}} \geq \theta, n \in U_k, q \neq k \,, \tag{18}$$

where θ is the interference-to-signal factor (ISF) threshold; $I_{q,n}$ is the interference power of user n from small cell q; $S_{k,n}$ is the received signal strength of user n from small cell k. The ISF threshold θ has the impact on the victimized user selection. Therefore, the effect of the ISF threshold θ for system energy efficiency is discussed in Section 7.3.

Fig. 4 shows that two small cells are deployed and multiple users communicate with a small cell. When $ISF_{1,2,7} \geq \theta$ and $ISF_{2,1,3} \geq \theta$, users 7 and 3 are regarded as the victimized users of small cells 1 and 2, respectively. If the high interference of victimized users can be eliminated, its throughput will be improved. In light of this, we first build

TABLE 5
Service-Victim (SV) Matrix for Two Small Cells Example

$SV(n,q)$	Small Cell 1	Small Cell 2
User 1	1	0
User 2	1	0
User 3	1	2
User 4	0	1
User 5	0	1
User 6	0	1
User 7	2	1

TABLE 6
The Initial Coverage User (CCU) Matrix in the Two Small Cells Example

$CCU(n,q)$	Small Cell 1	Small Cell 2
User 1	$B/\|C_1\|$	0
User 2	$B/\|C_1\|$	0
User 3	$B/\|C_1\|$	$B/\|C_1\|$
User 4	0	$B/\|C_2\|$
User 5	0	$B/\|C_2\|$
User 6	0	$B/\|C_2\|$
User 7	$B/\|C_1\|$	$B/\|C_2\|$

a service-victim (SV) matrix, which can identify the satisfactory users and the victimized users in each small cell. The initial SV matrix with all elements $SV(n,q)$ set to be zero. If user n is served by cell q, $SV(n,q) = 1$; If user n is a victimized user of cell q, $SV(n,q) = 2$. In this case, the SV matrix is shown in Table 5. Algorithm 1 shows the pseudocode for the SV matrix phase in a general case.

Algorithm 1. Victim-Aware Channel Rearrangement Algorithm (Phase 1)

```
phase 1: Service-victim (SV) matrix
for each user n do
    for each small cell q do
        if n ∈ U_q then
            SV(n,q) = 1
        else
            if I_{q,n}/S_{k,n} ≥ θ, n ∈ U_k, q ≠ k then
                SV(n,q) = 2
            else
                SV(n,q) = 0
            end if
        end if
    end for
end for
end phase 1
```

6.2 Phase 2: The Coverage User of Each Small Cell

The coverage users C_q contain the served users and the victimized users in small cell q. All the available bandwidth of each small cell can be equally split based on the number of the coverage users C_q. The allocated channel of the served users and the reserved channel of the victimized users are not overlapped in each small cell aiming to eliminate the interference for the victimized users. The initial channel rearrangement of coverage user (CCU) matrix with all elements $CCU(n,q)$ can be expressed as

$$CCU(n,q) = \frac{B}{|C_q|}, n \in C_q \,, \tag{19}$$

where B is the bandwidth of each small cell and $|C_q|$ is the number of coverage users of small cell q. Based on SV matrix, we can obtain the number of the coverage users of each small cell. Table 6 is the CCU matrix. The procedures of the initial CCU matrix phase are shown in Algorithm 2. Note that the same user can be simultaneously identified by multiple small cells as a victimized user. This user may

TABLE 7
The Updating CCU Matrix for the Victimized Users in the Two Small Cells Example

$CCU(n,q)$	Small Cell 1	Small Cell 2
User 1	$B/\|C_1\|$	0
User 2	$B/\|C_1\|$	0
User 3	$B/\|C_2\|$	$B/\|C_2\|$
User 4	0	$B/\|C_2\|$
User 5	0	$B/\|C_2\|$
User 6	0	$B/\|C_2\|$
User 7	$B/\|C_2\|$	$B/\|C_2\|$

TABLE 8
The Updating CCU Matrix for the Remaining Users in the Two Small Cells Example

$CCU(n,q)$	Small Cell 1	Small Cell 2
User 1	$B_{rem,1}/\|U_{rem,1}\|$	0
User 2	$B_{rem,1}/\|U_{rem,1}\|$	0
User 3	$B/\|C_2\|$	$B/\|C_2\|$
User 4	0	$B/\|C_2\|$
User 5	0	$B/\|C_2\|$
User 6	0	$B/\|C_2\|$
User 7	$B/\|C_2\|$	$B/\|C_2\|$

have unequal bandwidth. Phases 3 and 4 will make the final decision for the rearrangement channel for the victimized users and the non-victimized users, respectively.

Algorithm 2. Victim-Aware Channel Rearrangement Algorithm (Phase 2)

phase 2: The coverage user of each small cell
# of the coverage user of small cell q, $|C_q|$ is initialized to zero.
for each small cell q **do**
  for each user n **do**
    if $SV(n,q) = 1$ *or* 2 **then**
      $|C_q| = |C_q| + 1$
    end if
  end for
end for
The channel rearrangement of coverage user (CCU) matrix is initialized to zero matrix.
for each small cell q **do**
  for each user n **do**
    if $SV(n,q) = 1$ *or* 2 **then**
      $CCU(n,q) = \frac{B}{|C_q|}$
    end if
  end for
end for
end phase 2

6.3 Phase 3: The Channel Rearrangement of Victimized User

In the initial CCU matrix, user n may be assigned unequal bandwidth by different small cells q. As shown in Table 6, the channel of user 7 is initially reserved $\frac{B}{|C_1|}$ by small cell 1 and assigned $\frac{B}{|C_2|}$ by small cell 2. Because $|C_1| < |C_2|$, we obtain $\frac{B}{|C_1|} > \frac{B}{|C_2|}$. To eliminate the high interference for the victimized user 7 of small cell 1, the reserved channel of victimized user 7 is changed to a smaller $\frac{B}{|C_2|}$ in this phase. The reserved channel of victimized user 7 of small cell 1 and the allocated channel of the served user 7 of small cell 2 are set to the same channel. Based on the above discussion, Table 7 shows the updating CCU matrix. The details of the reserved channel of victimized user phase are shown in Algorithm 3.

6.4 Phase 4: The Channel Rearrangement of Remaining User

After phase 3, some small cells have the unused remaining channels. Table 7 shows that the allocated channel of the served user 3 in small cell 1 (i.e., the victimized user of the other small cell 2) becomes smaller. Also, the reserved channel of served user 7 of small cell 1 (i.e., the served user of the other small cell 2) is decreased. Small cell 1 has some unused channels. The coverage users of cell 1 can deduct its own victimized user and the interfering victimized user of other cells. Users 1 and 2 are the remaining users of small call 1. Updating allocated channel of the remaining user can be expressed as

$$CCU(n,q) = \frac{B_{rem,q}}{|U_{rem,q}|} = \frac{B_{rem,q}}{|C_q| - |U_{vic} \in C_q|}, n \in U_{rem,q}\ , \quad (20)$$

where U_{vic} is the set of the victimized users. In small cell q, $B_{rem,q}$ is the remaining channel after phase 3. $|U_{rem,q}|$ is the number of the remaining user. The remaining channels can be equally allocated to the remaining user. Further updating CCU matrix is given in Table 8. The pseudo code of channel rearrangement in the remaining user phase is shown in Algorithm 4.

Algorithm 3. Victim-Aware Channel Rearrangement Algorithm (Phase 3)

phase 3: The channel reservation of victimized user
The user n served and victimized by the set of the cells, G_n is initialized to empty set.
for each user n **do**
  for each small cell q **do**
    if $SV(n,q) > 0$ **then**
      $q \rightarrow G_n$, q becomes a member of G_n.
    end if
  end for
end for
Reserved channel of victimized user n is $min\{CCU(n,G_n)\}$
for each user n **do**
  for each small cell q **do**
    if $SV(n,q) > 0$ **then**
      $CCU(n,q) = min\{CCU(n,G_n)\}$.
    end if
  end for
end for
end phase 3

To summarize, the VACR mechanism results in the final CCU matrix to assign the adaptive channel for the connected users of small cell. The VACR mechanism can eliminate the interference of victimized users and guarantee QoS.

7 Performance Evaluation

We develop a DDRM framework, which can enhance the performance of UDSC in the complex and dynamic

TABLE 9
The Ultra-Dense Small Cells (UDSC) Network Parameters

Parameters	Value/Mode
Square area, a	2000 m^2
Density of small cell, λ_c	5000 $\mathrm{cells/km}^2$
Total small cell number, Q	10
Basic consumption of circuit for active mode, P_b	4800 mW
Basic consumption of circuit for sleeping mode, P_s	2900 mW
The power amplifier (PA) efficiency, Δ	8
The transmission power of reference signal, P_{ref}	17 dBm
Total bandwidth	20 MHz
Noise power density	-174 dBm/Hz
Shadowing standard deviation, σ_ψ	10 dB
Path loss exponent, α	3
Service type	Full buffer

scenarios. The DDRM framework starts from collecting data (e.g., RSRP). Then the resource management algorithms of the DDRM framework can determine the active/sleeping mode, the transmission power, and channel allocation. We perform simulation and show that the DDRM framework can improve the network performance of UDSC in different user densities. In each case, 1,000 iterations are implemented to generate various interference patterns. Therefore, we simultaneously consider dynamic cell switching on/off, cell transmission power control, channel rearrangement, time varying user density, and frequently changed interference for UDSC.

Algorithm 4. Victim-Aware Channel Rearrangement Algorithm (Phase 4)

phase 4: The channel rearrangement of remaining user
The available bandwidth of remaining users of small cell q, $B_{rem,q}$ is initialized to B.
U_{vic} is the set of victimized users.
G is the set of all small cells.
for each user n **do**
  if $sum\{SV(n,G)\} > 1, G = \{1,\ldots,q,\ldots,Q\}$ **then**
    $n \rightarrow U_{vic}$, n becomes a member of U_{vic}.
  end if
end for
for each small cell q **do**
  for each user n **do**
    if $n \in C_q$ *and* $n \in U_{vic}$ **then**
      $B_{rem,q} = B_{rem,q} - CCU(n,q)$
    end if
  end for
  for each user n **do**
    if $n \in C_q$ *and* $sum\{SV(n,G)\} = 1$ **then**
      $CCU(n,q) = \frac{B_{rem,q}}{|U_{rem,q}|} = \frac{B_{rem,q}}{|C_q| - |U_{vic} \in C_q|}$
    end if
  end for
end for
end phase 4

7.1 Parameters

Fig. 1 shows the considered simulation environment, in which small cells are randomly deployed in a square area a (i.e., 50 m $\times$ 40 m). In our simulation environment, Q = 10 small cells and the cell density is λ_c = 5,000 $\mathrm{cells/km}^2$. Moreover, the users are also randomly located in the same area. One small cell can connect multiple users. Table 9 shows the parameters adopted in our simulation. Referring to [31], [32], we assume that a small cell can have two modes of power consumption (i.e., active mode and sleeping mode). In the active mode, the basic circuit power is P_b = 4,800 mW and the PA efficiency is Δ = 8. In the sleeping mode, the basic circuit power is P_s = 2,900 mW. Furthermore, P_{ref} = 17 dBm [33]. We assume that small cells can share the total 20 MHz [34] and the system is fully loaded. All the channels are occupied by the users. We use the channel models as in [22]. Shadowing and path loss are the two radio propagation effects considered in our simulation. The shadowing component ψ is a log-normal random variable with standard deviation σ_ψ = 10 dB. The path loss exponent is α = 3.

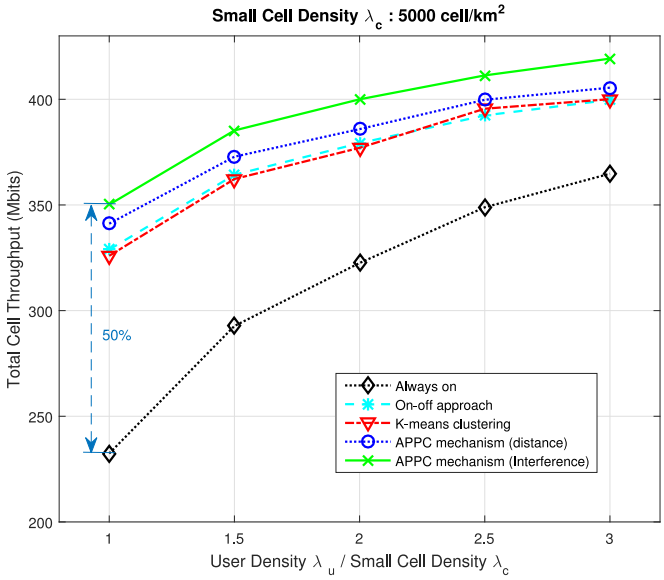

Fig. 5. The total cell throughput against the ratio of user density λ_u to small cell density λ_c using different power control approaches.

7.2 Comparison of Power Control Approaches

In this section, we compare the performance of the total cell throughput when applying various power control approaches: 1) always on (i.e., each cell with the maximum transmission power); 2) on/off power control approach; 3) K-means clustering based on distance; 4) APPC mechanism based on distance; and 5) APPC mechanism based on interference relationship. Fig. 5 shows the total cell throughput versus the ratio of user density λ_u to small cell density λ_c. The first power control approach (i.e., always on) presents all small cells with transmission power of 17 dBm. The second on/off power control approach means that the small cell can switch to the sleeping mode when a small cell does not serve any active user. The K-means clustering based on distance is illustrated in the following. The K-means clustering divides small cells into K clusters and finds K cluster centers. We choose the initial input parameter (i.e., the number of clusters) to be K = 2 for K-means clustering. The similarity values of K-means clustering are the negative squared Euclidean distance between two different small cells. In addition, the APPC mechanism based on distance means that the similarity values are set to the negative

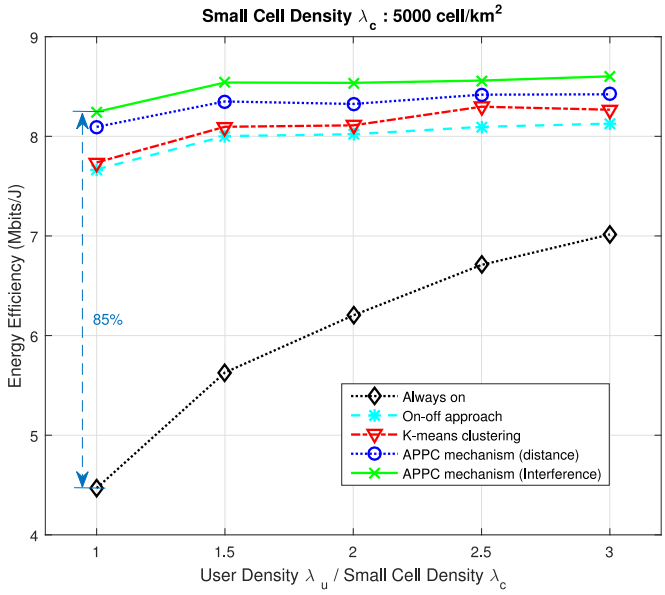

Fig. 6. The energy efficiency against the ratio of user density λ_u to small cell density λ_c using different power control approaches.

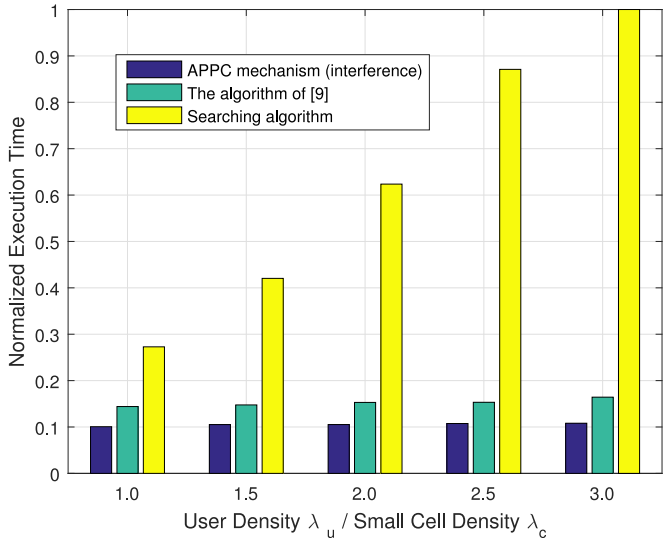

Fig. 7. The execution time of the APPC mechanism, the algorithm of [9], and the searching algorithm against λ_u/λ_c where the execution time is normalized to the longest execution time of the searching algorithm.

squared Euclidean distance between two different small cells. From the figure, we have the following observations:

1) Our proposed APPC mechanism based on interference performs the best among all the considered power control approaches. APPC can improve the total cell throughput by 50 percent compared to the baseline approach (i.e., always on) when $\lambda_u/\lambda_c = 1$. This is because our proposed approach can reduce the co-channel interference in the high density region.
2) The APPC mechanism based on distance ranks second, and has significant improvement compared to K-means clustering.
3) The K-means clustering based on distance performs the worst because of setting the number of clusters in advance and using the negative squared Euclidean distance as the similarity.

Fig. 6 shows the energy efficiency versus the ratio of user density λ_u to small cell density λ_c when various power control methods are implemented. The following phenomena are observed.

1) Compared to the baseline approach, the APPC mechanism based on interference can improve energy efficiency by 85 percent when $\lambda_u/\lambda_c = 1$.
2) We observe that increasing the ratio of user density λ_u to small cell density λ_c may slightly enhance the energy efficiency due to high power consumption except for the baseline approach.
3) Both APPC mechanisms based on interference and distance can perform better than the on/off approach for the various values of λ_u/λ_c. Hence, the APPC mechanism is crucial for the energy efficiency performance of UDSC.

In addition, we further compare the performance of the proposed APPC mechanism with the optimal solution based on the exhaustive searching algorithm. Furthermore, we compare APPC with a data-driven scheme that jointly considers the optimization of interference reduction and power saving [9]. Fig. 7 compares the execution time of the APPC mechanism, the algorithm of [9], and the searching algorithm against λ_u/λ_c. Here the execution time is normalized to the longest execution time of the searching algorithm. We observe that the execution time of the proposed APPC mechanism is the lowest among all the algorithms. The execution time of the exhaustive searching algorithm grows dramatically as λ_u/λ_c increases. Both the proposed APPC mechanism and the algorithm in [9] maintain about the same execution time as λ_u/λ_c increases. Fig. 8 shows the energy efficiency of the three aforementioned algorithms versus λ_u/λ_c. The proposed APPC mechanism and the algorithm of [9] can achieve 90 percent of the energy efficiency of the exhaustive searching algorithm in the case of $\lambda_u/\lambda_c = 3$ on average. More importantly, the unsupervised

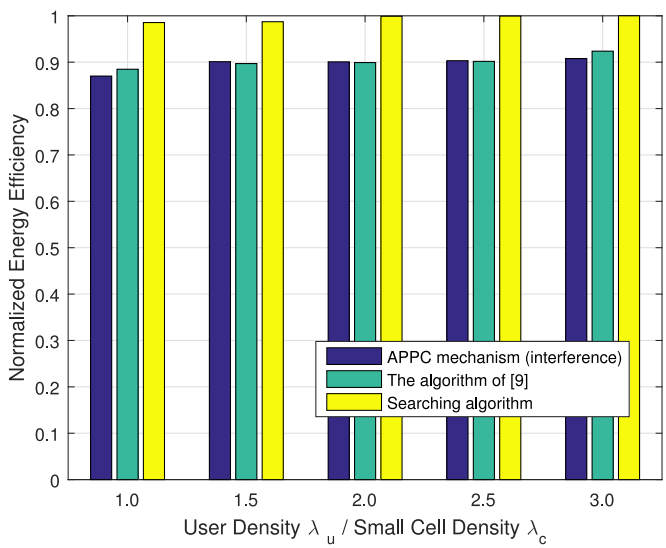

Fig. 8. The energy efficiency of the APPC mechanism, the algorithm of [9], and the searching algorithm against λ_u/λ_c where the energy efficiency is normalized to the largest energy efficiency of the searching algorithm.

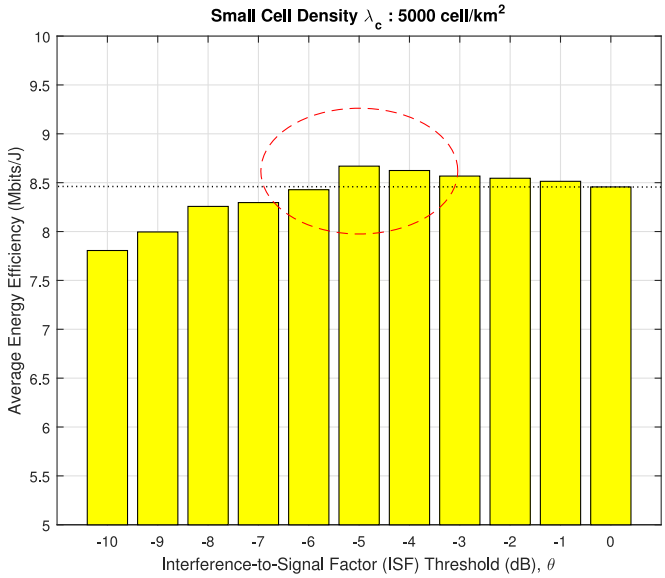

Fig. 9. The average energy efficiency of different interference-to-signal factor (ISF) threshold θ.

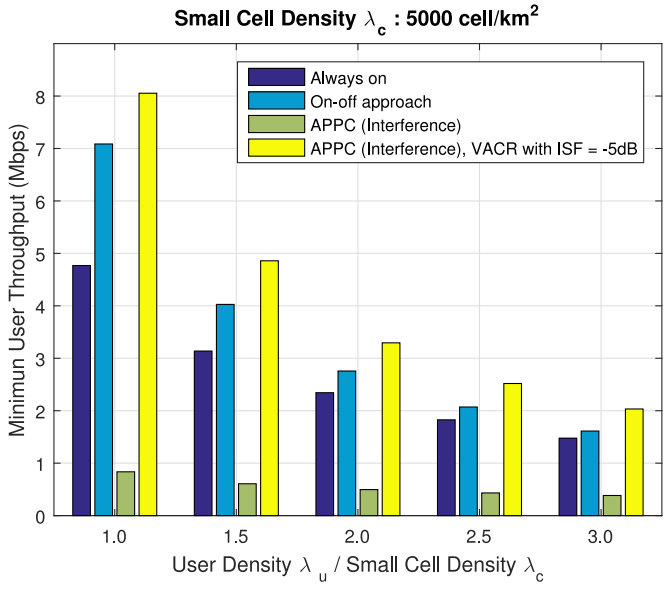

Fig. 10. The minimum user throughput against the ratio of user density λ_u to small cell density λ_c using different resource management approaches.

learning based APPC mechanism can be implemented without labeled data in a plug-and-play manner for UDSC. However, for the exhaustive searching algorithm and the algorithm of [9], the labeled system throughput is required with the corresponding configuration power level.

7.3 Effect of the Victim-Aware Channel Rearrangement (VACR) Mechanism

We further observe the benefits of the VACR mechanism for UDSC. We first conduct an experiment to validate the impact of ISF threshold θ. Fig. 9 shows the average energy efficiency of UDSC for various ISF threshold θ in our proposed DDRM framework. The average energy efficiency can be inferred by the mean of energy efficiency in various values of λ_u/λ_c. For $\theta = 0$ dB, the small cells only execute the APPC mechanism without considering channel rearrangement. From the figure, we observe the following:

1) The lower the ISF threshold θ, the more the victimized users. Thus, fewer channels can be used for the remaining users. Hence, if ISF threshold θ (i.e., smaller than $\theta = -5$ dB), the average energy efficiency gradually declines due to the reduced total cell throughput.
2) The VACR mechanism with the ISF threshold $\theta = -5$ dB has better performance than other ISF threshold values. Compare the ISF threshold $\theta = 0$ dB (i.e., only APPC mechanism based on interference), the case of $\theta = -5$ dB can maintain nice average energy efficiency of UDSC.

Fig. 10 shows the minimum user throughput in the system versus the ratio of λ_u/λ_c for various power control approaches when adopting VACR mechanism with $\theta = -5$ dB. From the figure, we have the following observations:

1) Appending the joint APPC and VACR mechanisms can improve 70 percent of the minimum user throughput over the baseline always on approach when the ratio is $\lambda_u/\lambda_c = 1$.
2) The APPC mechanism based on interference cannot guarantee QoS for every user because the user throughput degrades at the cell edge due to power adjustment of the serving cell.
3) Compared to the APPC mechanism based on interference, appending the VACR mechanism can significantly improve the minimum user throughput. This result implies that the VACR mechanism can be used to satisfy QoS for each user in the UDSC.

To further discuss the transmission link reliability of active users, we consider the link reliability $L_{rel} = 90\%$. Table 10 shows the link reliability performance of the DDRM framework with APPC and VACR mechanisms in comparison with the baseline always on approach. In a LTE system, each user can be assigned the appropriate modulation and coding scheme (MCS) based on the SINR value [35]. Nevertheless, different users connected to the same cell can be assigned to distinct MCS [36]. Note that the link reliability performance of the baseline approach can achieve 90 percent or higher in the QoS constraint requirement

TABLE 10
The Transmission Link Reliability for Various the Ratios of User Density λ_u to Small Cell Density λ_c

λ_u/λ_c	MCS	Modulation	Code Rate	SINR Threshold [dB] Γ_{th}	Always On Link Reliability L_{rel}	APPC, VACR Link Reliability L_{rel}
1.0	MCS2	QPSK	1/9	-4	94.70%	100.00%
	MCS6	QPSK	3/5	3	40.84%	95.42%
1.5	MCS2	QPSK	1/9	-4	94.14%	100.00%
	MCS6	QPSK	3/5	3	42.28%	91.68%
2.0	MCS2	QPSK	1/9	-4	94.18%	100.00%
	MCS5	QPSK	1/2	1	55.16%	97.07%
2.5	MCS2	QPSK	1/9	-4	93.91%	100.00%
	MCS5	QPSK	1/2	1	54.62%	95.96%
3.0	MCS2	QPSK	1/9	-4	94.29%	100.00%
	MCS5	QPSK	1/2	1	55.04%	91.43%

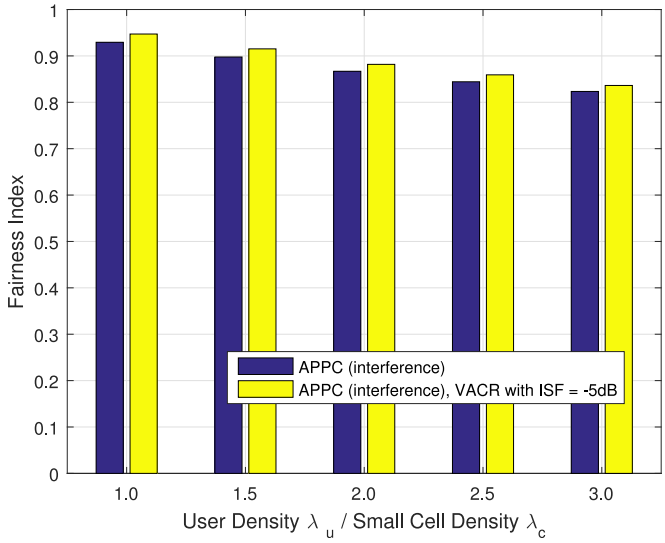

Fig. 11. The fairness index against the ratio of user density λ_u to small cell density λ_c.

$\Gamma_{th} = -4$ dB (i.e., MCS index is 2). Second, when $\Gamma_{th} = 3$ dB (i.e., MCS index is 6) is considered, the link reliability performance of our proposed DDRM framework can achieve 90 percent only for lower ratio λ_u/λ_c. Therefore, the DDRM framework with APPC and VACR mechanisms not only can enhance the energy efficiency but can guarantee link reliability for each user.

Inaddition, the edge users of the cluster centers have low signal strength after the cluster centers lower their transmission power by the APPC mechanism. The edge users of the cluster centers also suffer from strong interference from other cells. The victimized users are defined as the ones with low signal strength and high interference. Thus, the edge users of the cluster can be considered to be victims. The proposed VACR mechanism can compensate the victimized users. We use Jain's fairness index [23] to measure the fairness in terms of user throughput in the cluster center. As shown in Fig. 11, the average fairness index of cluster centers under the joint APPC and VACR mechanisms is slightly higher than that under the APPC mechanism. Therefore, the channel rearrangement mechanism can maintain users' fairness.

8 Conclusion

The deployment of UDSC can improve system capacity and service coverage to meet the tremendous growth of mobile service requirements, specially for hotspots and indoor environments. We propose a joint cell switching on/off, transmission power control and channel rearrangement to improve the total system energy efficiency. We consider the effects of non-uniformly distributed traffic loads and frequently changing interference. The theoretical analysis of the considered problem is challenging. Therefore, we propose the DDRM framework to solve this issue. We demonstrated that in complex UDSC the energy consumption and serious interference can be efficiently controlled by utilizing the collected operation data, such as RSRP from user's devices, the number of serving users and transmission power per cell, and so on. We find that the affinity propagation clustering interference reduction can help understand complicated interference in the pull-and-play ultra-dense small cells, which requires neither prior knowledge nor labeled data. We developed the DDRM framework to take the input data (i.e., collected operation data) for APPC mechanism to select the proper cells to adjust transmission power. Then we designed the VACR mechanism to ensure the QoS of the edge users. Our simulation results show that our proposed approaches can improve the performance of UDSC significantly under an environment of complicated interference and dynamical traffic variations. In the future, the proposed data-driven radio resource management framework can be extended to investigating fast handover and cross-tier interference in the heterogeneous networks.

Acknowledgments

This work was sponsored by the Ministry of Science and Technology (MOST) of Taiwan under grants MOST 107-2634-F-009-006.

References

[1] M. Ismail, "Mitigating inter-cell interference in 5G ultra-dense femtocell networks: Issues and challenges," in *Proc. IEEE Student Conf. Res. Develop.*, Dec. 2016, pp. 1–2.
[2] K. H. Lin, C. H. Tsai, J. W. Chang, Y. C. Chen, H. Y. Wei, and F. M. Yeh, "Max-throughput interference avoidance mechanism for indoor self-organizing small cell networks," *Inf. Commun. Technol. Express*, vol. 3, pp. 132–136, May 2017.
[3] C. Yang, J. Li, and M. Guizani, "Cooperation for spectral and energy efficiency in ultra-dense small cell networks," *IEEE Wireless Commun.*, vol. 23, no. 1, pp. 64–71, Feb. 2016.
[4] C. Yang, J. Li, Q. Ni, A. Anpalagan, and M. Guizani, "Interference-aware energy efficiency maximization in 5G ultra-dense networks," *IEEE Trans. Commun.*, vol. 65, no. 2, pp. 728–739, Feb. 2017.
[5] J. Zheng, Y. Wu, N. Zhang, H. Zhou, Y. Cai, and X. Shen, "Optimal power control in ultra-dense small cell networks: A game-theoretic approach," *IEEE Trans. Wireless Commun.*, vol. 16, no. 7, pp. 4139–4150, Jul. 2017.
[6] M. Kulin, C. Fortuna, E. D. Poorter, D. Deschrijver, and I. Moermans, "Data-driven design of intelligent wireless networks: An overview and tutorial," *Sensors*, vol. 16, Jun. 2016, Art. no. 790.
[7] A. Imran and A. Zohas, "Challenges in 5G: How to empower SON with big data for enabling 5G," *IEEE Netw.*, vol. 28, no. 6, pp. 27–33, Nov. 2014.
[8] C. Jiang, H. Zhang, Y. Ren, Z. Han, K. C. Chen and L. Hanzo, "Machine learning paradigms for next-generation wireless networks," *IEEE Wireless Commun.*, vol. 24, no. 2, pp. 98–105, Apr. 2017.
[9] L. C. Wang, S. H. Cheng, and A. H. Tsai, "Bi-SON: Big-data self organizing network for energy efficient ultra-dense small cells," in *Proc. IEEE 84th Veh. Technol. Conf.*, Sep. 2016, pp. 1–5.
[10] S. Falangitis, P. Spapis, P. Magdalinos, G. Beinas, and N. Alonistioti, "Clustering for small cells," in *Proc. Eur. Conf. Netw. Commun. (EuCNC)*, 2014, pp. 1–5.
[11] B. J. Frey and D. Dueck, "Clustering by passing messages between data points," *Sci.*, vol. 315, pp. 972–976, Feb. 2007.
[12] L. C. Wang, S. H. Cheng, and A. H. Tsai, "Data-driven power control of ultra-dense femtocells: A clustering based approach," in *Proc. IEEE Wireless Opt. Commun. Conf.*, Apr. 2017, pp. 1–6.
[13] Y. Zhang, S. Wang and J. Guo, "Clustering-based interference management in densely deployed femtocell networks," in *Proc. IEEE/CIC Int. Conf. Commun. China*, Nov. 2015, pp. 1–6.
[14] S. Fan, J. Zheng and J. Xiao, "A clustering-based downlink resource allocation algorithm for small cell networks," in *Proc. Int. Conf. Wireless Commun. Signal Process.*, Oct. 2015, pp. 1–5.
[15] J. Qiu, G. Ding, Q. Wu, Z. Qian, T. A. Tsiftsis, Z. Du, and Y. Sun, "Hierarchical resource allocation framework for hyper-dense small cell networks," *IEEE Access*, vol. 4, pp. 8657–8669, Nov. 2016.
[16] I. Shgluof, M. Ismail, and R. Nordin, "Semi-clustering of victim-cells approach for interference management in ultra-dense femtocell networks," *IEEE Access*, vol. 5, pp. 9032–9043, Apr. 2017.

[17] W. Li, W. Zheng, Y. Xie, and X. Wen, "Clustering based power saving algorithm for self-organized sleep mode in femtocell networks," in *Proc. 15th Int. Symp. Wireless Pers. Multimedia Commun.*, Sep. 2012, pp. 379–383.
[18] A. U. Ahmed, M. T. Islam, M. Ismail, S. Kibria, and H. Arshad, "A novel user classification method for femtocell network by using affinity propagation algorithm and artificial neural network," *The Sci. World J.*, vol. 2014, Jul. 2014, Art. no. 253787.
[19] *Evolved Universal Terrestrial Radio Access (E-UTRA) and Evolved Universal Terrestrial Radio Access Network (E-UTRAN); Overall description; Stage 2 (Release 14)*, document TS 36.300, 3GPP, Jul. 2017. [Online]. Available: http://www.etsi.org/deliver/etsi_ts/136300_136399/136300/14.03.00_60/ts_136300v140300p.pdf
[20] Y. L. Lee, J. Loo, T. C. Chuah, and A. A. El-Saleh, "Fair resource allocation with interference mitigation and resource reuse for LTE/LTE-A femtocell networks," *IEEE Trans. Veh. Technol.*, vol. 65, no. 10, pp. 8203–8217, Oct. 2016.
[21] T. X. Brown, "Cellular performance bounds via shotgun cellular systems," *IEEE J. Sel. Areas Commun.*, vol. 18, no. 11, pp. 2443–2455, Nov. 2000.
[22] *Technical Specification Group Radio Access Network; Evolved Universal Terrestrial Radio Access (E-UTRA); Further advancements for E-UTRA physical layer aspects (Release 9)*, document TR 36.814, 3GPP, Mar. 2010. [Online]. Available: http://www.qtc.jp/3GPP/Specs/36814-900.pdf
[23] X. L. Wu, W. J. Zhao, and W. Wu, "Throughput and fairness-balanced resource allocation algorithm in TD-LTE-advanced relay-enhanced network," in *Proc. Int. Workshop High Mobility Wireless Commun.*, 2013, pp. 82–86.
[24] *Technical Specification Group Radio Access Network; Small cell enhancements for E-UTRA and E-UTRAN - Physical layer aspects (Release 12)*, document TR 36.872, 3GPP, Dec. 2013. [Online]. Available: http://www.tech-invite.com/3m36/tinv-3gpp-36-872.html
[25] E. Ternon, P. K. Agyapong, and A. Dekorsy, "Performance evaluation of macro-assisted small cell energy savings schemes," *Wireless Commun. Netw.*, vol. 2015, Sep. 2015, Art. no. 209.
[26] Z. Chen and Y. Tang, "A resource collaboration scheduling scheme in ultra-dense smallcells," in *Proc. Int. Conf. Comput. Sci. Edu.*, 2017, pp. 401–405.
[27] O. G. Aliu, A. Imran, M. A. Imran, and B. Evans, "A survey of self organisation in future cellular networks," *IEEE Commun. Surveys Tut.*, vol. 15, no. 1, pp. 336–361, Jan.–Mar. 2013.
[28] S. Xiongkai, P. Jing, and L. Jianzhou, "A method of dynamically determining the number of clusters and cluster centers," in *Proc. Int. Conf. Comput. Sci. Edu.*, Apr. 2013, pp. 283–286.
[29] Y. Zhu, J. Yu and C. Jia, "Initializing K-means clustering using affinity propagation," in *Proc. 9th Int. Conf. Hybrid Intell. Syst.*, Aug. 2009, pp. 338–343.
[30] P. Thavikulwat, "Affinity propagation: A clustering algorithm for computerassisted business simulations and experiential exercises," in *Proc. Developments Bus. Simul. Experiential Learning*, vol. 35, pp. 220–224, 2008.
[31] G. Auer, V. Giannini, C. Desset, I. Godor, P. Skillermark, M. Olsson, M. Imran, D. Sabella, M. Gonzalez, O. Blume, and A. Fehske, "How much energy is needed to run a wireless network?" *IEEE Wireless Commun.*, vol. 18, no. 5, pp. 40–49, Oct. 2011.
[32] R. Bonnefoi, C. Moy, and J. Palicot, "Dynamic sleep mode for minimizing a femtocell power consumption," in *Proc. Int. Conf. Cogn. Radio Oriented Wireless Netw.*, May 2016, pp. 618–629.
[33] S. Aerts, D. Plets, A. Thielens, L. Martens, and W. Joseph, "Impact of a small cell on the RF-EMF exposure in a train," *Int. J. Environ. Res. Public Health*, vol. 12, pp. 2239–2252, 2015.
[34] C. Bouras and G. Diles, "Sleep mode performance gains in 5G femtocell clusters," in *Proc. Int. Congress Ultra Modern Telecommun. Control Syst. Workshops*, 2016, pp. 141–146.
[35] J. Fan, Q. Yin, G. Y. Li, B. Peng, and X. Zhu, "MCS selection for throughput improvement in downlink LTE systems," in *Proc. Int. Conf. Comput. Commun. Netw.*, Aug. 2011, pp. 1–5.
[36] D. L. Perez, A. Ladanyi, A. Juttner, H. Rivano, and J. Zhang, "Optimization method for the joint allocation of modulation schemes, coding rates, resource blocks and power in self-organizing LTE networks," in *Proc. Int. Conf. Comput. Commun. Netw.*, Apr. 2011, pp. 111–115.

Li-Chun Wang (M'96-SM'06-F'11) received the BS degree from National Chiao Tung University, Taiwan, R. O. C. in 1986, the MS degree from National Taiwan University in 1988, and the Ms Sci and PhD degrees from the Georgia Institute of Technology, Atlanta, in 1995, and 1996, respectively, all in electrical engineering. From 1990 to 1992, he was with the Telecommunications Laboratories of the Ministry of Transportations and Communications in Taiwan. In 1995, he was affiliated with Bell Northern Research of Northern Telecom, Inc., Richardson, TX. From 1996 to 2000, he was with AT&T Laboratories, where he was a Senior Technical Staff Member in the Wireless Communications Research Department. Since August 2000, he has joined National Chiao Tung University in Taiwan. Currently he is a chair professor of the Department of Electrical and Computer Engineering and is jointly appointed by the Department of Computer Science. His recent research interests are focused on cross-layer optimization and data-driven learning techniques for 5G ultra-reliable and ultra-low latency communications (URLLC), edge computing, unmanned aerial vehicle (UAV) communications networks, and AI-empowered mobile networks. He was elected to the IEEE Fellow for his contributions in cellular architectures and radio resource management in wireless networks. He won the 1997 IEEE Jack Neubauer Best Paper Award (1997), Distinguished Research Award of Ministry of Science and Technology, Taiwan (2012 and 2018), and IEEE Communications Society Asia-Pacific Board Best Paper Award (2015). He has published over 90 journal papers and 180 conference papers, 19 US patents and co-edited a book Key Technologies for 5G Wireless Systems (Cambridge 2016).

Shao-Hung Cheng received the BS and MS degrees from the Department of Applied Physics, Chung Cheng Institute of Technology, National Defense University, Taiwan, in 2005 and 2008, respectively. He is currently working toward the PhD degree in the Department of Electrical and Computer Engineering, National Chiao Tung University, Taiwan. From 2013 to 2014, he was a lecturer with the Department of Electrical and Electronic Engineering, Chung Cheng Institute of Technology, National Defense University. His research interests include wireless communication, radio resource management in small cell networks, self-optimization and machine learning. He is a student member of the IEEE.